Adsorption (2013) 19:1149–1163
DOI 10.1007/s10450-013-9543-2

Intrinsic adsorption properties of CO_2 on 5A and 13X zeolite

Qassim Hassan Dirar · Kevin F. Loughlin

Received: 12 May 2012 / Accepted: 12 March 2013 / Published online: 5 April 2013

Abstract Data for the adsorption of CO_2 on 5A (CaA) and 13X (NaX) zeolite are critically evaluated. In addition, fresh data for the adsorption of CO_2 on 13X zeolite is reported. Three intrinsic properties are examined: q_{max}, the saturation loading, K_H, the Henry constant, and $(-\Delta H)_q$, the isosteric heat of sorption. Below a reduced temperature T_r, of 0.9, the q_{max} values for both 5A and 13X zeolites are similar to theoretical values that may be derived using zeolitic crystallographic properties and the sorbate density calculated using the Rackett equation. For the region $0.9 \leq Tr \leq 1.0$, the calculated q_{max} values exceed the theoretical values similarly calculated, indicating that the molecules have a smaller molar volume than in a similar liquid phase. This is a similar result to that observed in ionic liquids. Linear regressed equations are derived for q_{max} for the region $0.9 \leq Tr \leq 1.25$. The Henry constant values for 5A are remarkably consistent for the five studies examined, with a correlation coefficient, R, of 0.999 for the van't Hoff equation, but for the seven studies examined in 13X the data is more disperse as indicated by a correlation coefficient R of 0.899 for the van't Hoff equation. The values of $(-\Delta H)_q$, the isosteric heat of sorption are in agreement with the literature. An explanation is advanced for the discrepancy between the higher heats of sorption values obtained calorimetrically from those obtained from isosteric adsorption studies. Finally, the fresh data is observed to fit the Toth model with regression coefficients of 0.999. However, the parameters obtained for the Toth equation by regression are significantly different from the intrinsic properties derived earlier, indicating the difficulty of deriving intrinsic parameters from isotherm fits.

Keywords Carbon dioxide · 5A · 13X · Maximum loading · Henry constant · Isosteric heat

Electronic supplementary material The online version of this article (doi:10.1007/s10450-013-9543-2) contains supplementary material, which is available to authorized users.

Q. H. Dirar · K. F. Loughlin (✉)
Department of Chemical Engineering, American University of Sharjah, P.O. Box 26666, University City, Sharjah, UAE
e-mail: kloughlin@aus.edu; b00018125@alumni.aus.edu

List of symbols

Variables

a	Zeolite cell width (pm)
A_i	Coefficients in virial isotherm
b	Parameter in Toth eqt. (kPa^t)
M	Atomic mass unit of cell
MW	Molecular weight of adsorbate
K_H	Henry constant (g/100 g Z kPa)
K_0	Pre-exponential factor in van't Hoff eqt. (g/100 g Z kPa)
N_0	Avogadro's number
P_c	Critical pressure (kPa)
q_{max}	Maximum zeolite loading (g/100 g Z)
q^*_{max}	Maximum adsorbent loading, g/100 g adsorbent
q_{st}	Isosteric heat at various loadings (kJ/mol)
R	Gas constant (kPa.cc/gmol K)
T_c	Critical temperature (K)
T_r	Reduced temperature
V_A	Sorbate volume (cc/g or cc/mol)
V_c	Critical volume (cc/g)
V_{sat}	Saturated liquid volume (cc/g)
Z	Formula weight for cell
Z_c	Critical compressibility
ZRA	Rackett parameter

Greek Letters

α	A cage in 5A zeolite, 776 $Å^3$
β	β cage in both zeolites, 150 $Å^3$

$-\Delta H_0$	Heat of adsorption at zero loading, kJ/mol
ε_Z	Large or α cage crystallographic zeolite void volume for all molecules except water and ammonia, 0.455 cc/cc for NaX, 0.387 cc/cc for 5A
θ	Loading, at saturation = 1
ρ_{sat}	Sorbate liquid density, g adsorbate/cc
ρ_Z	Zeolite crystallographic density, 1.43 g/cc, for NaX, 1.48 g/cc for 5A
ω	Fraction of 5A zeolite crystals in the adsorbent

1 Introduction

Concern over climate warming and the need for sequestration of carbon dioxide has resulted in many studies of the adsorption of carbon dioxide on 5A and 13X zeolite. Recently Llano-Restrepo (2010) comprehensively reviewed the literature for the adsorption of CO_2 on NaX (13X) zeolite. His primary purpose was to model the isotherms using a generalized statistical thermodynamic adsorption model (GTSA) and derive the isosteric heats of adsorption. For this, he used the data of Pulin et al. as his source (Pulin 2001). He also provides structural interpretation of the adsorption of CO_2 on the NaX zeolite. His work can be criticized as the number of parameters required to model the GTSA isotherms is large, well over 6, more likely 12 when the pre-exponential factors and heats of adsorption are included. Secondly, he has only used one set of data for his modeling purposes although there are many sets of data available in the literature. Thirdly, the values of q_{max}/(g/100 g Z) used are rather large as will be observed. A similar comprehensive review of the adsorption of CO_2 on 5A zeolite is not available, particularly for high pressure adsorption data.

In this study, the authors had the following objectives:

- Present fresh data for the adsorption of CO_2 on 13X zeolite.
- Model the q_{max} saturation loading of CO_2 for both 5A and 13X zeolites using available literature data.
- Determine the intrinsic Henry constants for both 5A and 13X zeolites using multiple studies from the literature.
- Derive the isosteric heat of sorption of CO_2 on both 5A and 13X zeolites as a function of loading for multiple studies,
- Model the fresh data for CO_2 on 13X zeolite using the Toth isotherm. The results of this modeling are compared with the intrinsic values of q_{max} and Henry constants calculated earlier.

An intrinsic property is defined as a fundamental adsorbate-adsorbent interaction uninfluenced by a secondary variable. The traditional means of calculating parameters for an adsorption model using an isotherm such as Langmuir's, results in an interaction between the Henry constant and the saturation loading. This limits the intrinsic nature of the resulting parameters. The objectives listed above have as their goal the search for the fundamental nature of the adsorbate-adsorbent system.

The literature was systematically searched for high concentration carbon dioxide data; low pressure data and calorimetric data were also collected. Tabulated data was saved in EXCEL files. Untabulated data for CO_2 adsorption on NaX (13X) and CaA (5A) are extracted from literature papers by digitizing the appropriate Figures and then saving in EXCEL FILES. In general, high pressure loading data is scarce when compared to studies at low to moderate pressure. Fourteen studies were analyzed for zeolite 13X in which six contained high pressure data (Avgul 1968; Brandani 2003; Cavenati et al. 2004; Burgess 1989; Hyun 1982; Wang and LeVan 2009; Pulin 2001; Shen 1998; Shen et al. 2000; Dunne et al. 1996). Four of the 14 studies are not included as the binder content is unspecified. Similarly, nine studies were analyzed for zeolite 5A in which only three contained high pressure data (Brandani 2003; Chen 1990; Pakseresht 2002, Wang and LeVan 2009; Wang et al. 1998; Saha et al. 2009). Again, four had unspecified binder content. The low pressure data is useful for extracting the Henry constants, and all the data is useful for extracting the isosteric heat of sorption.

2 Theory

The theoretical saturation loading in 13X and 5A zeolites may be calculated from first principles for zeolite crystals as:

$$q_{max} = 100\frac{\rho_{sat}\in_Z}{\rho_Z} \tag{1}$$

where ρ_{sat} is the saturation density of the adsorbate, $\in_Z$ is the zeolite crystal porosity, and ρ_Z is the zeolite density. For molecular sieves containing a fraction ω of crystals with a fraction (1 − ω) of binder, a factor of ω is used to relate the reported loading based on adsorbent q^*_{max} to that based on crystals.

$$q_{max} = \left(\frac{1}{\omega}\right)q^*_{max} \tag{2}$$

In these equations, the saturation density for liquids below the critical point is calculated using either the modified Rackett equation:

$$V_{sat} = \frac{1}{\rho_{sat}} = \left(\frac{RT_C}{P_C MW}\right)ZRA^{\left[1+(1-T_r)^{0.2857}\right]} \tag{3}$$

where R is the universal gas constant, T_c is the critical temperature, P_c is the critical pressure, MW is the

molecular weight, *ZRA* is the Rackett parameter, and T_r is the reduced temperature or the Rackett equation:

$$V_{sat} = \frac{1}{\rho_{sat}} = V_C Z_C^{(1-T_r)^{0.2857}} \quad (4)$$

where V_C is the critical volume, Z_C is the critical compressibility, and T_r is the reduced temperature.

Substituting Eq. 3 in Eq. 1 gives

$$q_{max} = 100\frac{\in_Z}{\rho_Z}\left(\frac{P_C MW}{RT_C}\right) ZRA^{-\left[1+(1-T_r)^{0.2857}\right]} \quad (5)$$

The value of *ZRA* is 0.2736 for carbon dioxide (Spencer and Danner 1972). The values of ε_Z and ρ_Z may be found in Breck's text (1974). However, the authors were unclear as to the specific meaning of the properties in his Tables (Tables 2.18 and 2.63]; accordingly the parameters were recalculated from first principles.

For the hydrated crystal of NaX in Breck's text (1974), the properties are itemized in Table 1; the formula weight given is $Na_{86}[(AlO_2)_{86}(SiO_2)_{106}]\cdot 264H_2O$. Assuming covalent bonding, the atomic volume for the solid structure $Na_{86}[(AlO_2)_{86}(SiO_2)_{106}]$ is itemized for each atom in Table 2; similarly the atomic volume of the water of hydration is itemized. The total solid volume and the total volume of the occluded water is calculated.

The derived properties for the crystal are presented in Table 3. The unit cell volume is calculated using 25 Å as the X-ray crystallographic width (Breck 1974). The fraction solids, fraction water, and the excluded volume are then calculated. Excluded volume is that volume of the zeolite lattice unavailable for adsorption of molecules, due to closest approach of sorbate molecules to the zeolite lattice. As water is occluded in both the β and large cages, the excluded fractional volume of 0.28 is the volume unavailable to water due to the repulsion forces between the crystal lattice and the occluded water.

The derived properties of the crystal are presented in Table 3 assuming a cubic lattice with a dimension of 25 $Å^3$ (Breck 1974). In the case of water which is adsorbed in both the large and β cages, the cell may be divided into three fractions: (i) the fraction solids (0.215), (ii) the fraction water (0.505), and (iii) the fraction of excluded volume which is 0.280 (1-0.215-0.505). The fractional volume of the β cage [≡ 8 × 151 Å (volume of sodalite cage of diameter 6.6 Å in Breck's text)] is 0.077. Therefore the fractional volume of the large cage is 0.708 (1-0.215-0.077). The fractional void volume is 0.785 (0.708 + 0.077) but 0.280 is excluded volume leaving 0.505 (0.708 + 0.077–0.280) fraction for adsorption of water, similar to the void volume reported by Breck in Table 2.18 (1974). In the case of large molecules, the β cage is inaccessible as only NH_3 and H_2O can access this cage. As the excluded fractional volume 0.280 represents

Table 1 Recalculation of properties of zeolite 13X from Breck's[3] text

Chemical composition	
Typical unit cell contents	$Na_{86}[(AlO_2)_{86}(SiO_2)_{106}].264H_2O$
Variations	Si/Al = 1–1.5
Crystallographic data	
Symmetry	Cubic
Density	1.93 g/cc
Unit cell constants	a = 25.02 − 24.86 Å; X-ray powder data
Unit cell volume	15,362–15,670 $Å^3$
Structural properties	
Void volume	0.50 cc/cc
Framework density	1.31 g/cc
Free aperture	12-ring, 7.4 Å; 6-ring 2.2 Å
Largest molecule admitted to 12 ring	$(C_4H_9)_3N$; kinetic diameter, is 8.1 Å
Largest molecule admitted to 6 ring (from page 636)	H_2O; kinetic diameter, is 2.65 Å

[a] Data source is Table 2.63 in Breck's text

Table 2 Basic building units for $Na_{86}[(AlO_2)_{86}(SiO_2)_{106}]\cdot 264H_2O$ zeolite

Specie	Atomic mass	n	Covalent radius/pm	Atomic volume/pm^3	Atomic volume/m^3	Total volume/m^3
Dehydrated crystal						
Si	28.086	106	111	5.729E+06	5.729E−30	6.072E−28
O	15.999	384	66	1.204E+06	1.2049E−30	4.624E−28
Al	26.982	86	121	7.421E+06	7.421E−30	6.382E−28
Na	22.99	86	166	1.916E+07	1.916E−29	1.648E−27
Total Solid Volume/m^3						3.356E−27
Hydrated crystal						
H_2O	18.01	264	4754.788	2.991E+07	2.991E−29	7.895E−27
Total volume (Solid + Occluded Water)/m^3						1.125E−26

Table 3 Derived properties from the basic building units for 13X & 5A zeolites

Property	13X	5A
Unit cell volume, a^3/m^3	1.563E−26	1.870E−27
Fraction solids puc	0.215	0.223
Fraction water puc	0.505	0.432
Fraction excluded volume puc	0.280	0.345
Volume (large or α cage) puc/m^3	1.210E−27	1.510E−28
Fractional volume β cage puc	0.077	0.081
Fractional volume large cage	0.708	0.696
Fractional void volume (β + large or α cage)	0.785	0.777
Fractional void volume (occluded) total cell	0.505	0.432
Fractional void volume (occluded) (large or α cage)	0.455	0.387
Framework density (g/cm^3)	1.43	1.48
Moles in 1 cc [= ρ/MW(MW = cell atomic mass)]	1.066E−04	8.863E−04
Cells in 1 cc (= moles[a] N_0)	6.418E+19	5.340E+20
Conversion factor (molecule puc)/(mmole/g)	13.420	NA
Conversion factor for 1/8th of cell	1.68	1.67[a]

Data source for 5A data is Table 2.18 in Breck's text

[a] Note the value typically used in the literature is 1.78

35.67 % of the free volume, the occluded fractional volume for the large cage is 0.455 [0.708 × (1 − 0.357)].

The framework density for the dehydrated zeolite is calculated using the equation (www.tutorvista.com 2011)

$$\rho = \frac{Z * M}{a^3 N_0 10^{-30}} \tag{6}$$

where Z is the formula unit (= 1 puc), M is the atomic mass unit of the cell, a/pm is the cell width and N_0 is Avogadro's number (6.02257 × 10^{23}). The framework density is found to be 1.43 g/cm^3, similar to that calculated by Dubinin and Astakhov (1971) but different from the value of 1.31 g/cm^3 given in Breck's book. Finally the conversion factor from mmoles/g to molecules *puc* may be calculated from

$$1 molecule puc = 1 \frac{molecule}{cell} \frac{\#cells}{cm^3} \frac{1}{\rho} \frac{ccm^3}{g} \frac{1}{N_0} \frac{mole}{molecules} \frac{1000\ mmole}{mole} \left(\frac{mmole}{g}\right) \tag{7}$$

and is presented in the last two lines of Table 3.

Calculations are also given for the 5A cell in Table 3 for the formula weight of $Na_{12}[(AlO_2)_{12}(SiO_2)_{12}]\cdot 27H_2O$ which is the pseudo cell. The excluded volume is 34.5 % for 5A, which is higher than the 28 % excluded volume for the 13X zeolite. This is a reflection of the smaller large cavity in the 5A type zeolite. The occlusion volume is 43.2 % for the unit cell of 5A for water and ammonia, but is only 38.7 % for all other sorbates as they are unable to access the β cage in the 5A zeolite. The occlusion volume for water and framework density are 0.432 and 1.48 g/cm^3 different from Breck's values of 0.47 and 1.27 g/cm^3 [Table 2.18, (Breck 1974)]. However, the fractional occlusion volume for larger molecules is only 0.387 as the β cage is inaccessible to them. Steric effects may increase the size of the excluded volumes for other sorbates.

To interpret the intrinsic Henry constant from experimental data, it is desirable that data be measured in the low concentration region where θ, the fractional coverage, is <0.5. However this is very seldom achieved particularly at temperatures below a reduced temperature of 0.8 as the isotherms tend to be highly rectangular under these conditions. To take into account all the available data, it is desirable to use a model isotherm applicable over a wide span of concentrations. Most models have two or more parameters including K_H and θ, among their parameter list. However, frequently an interaction is observed to occur between the derived values of K_H and θ, reducing the level of confidence in each parameter, and possibly invalidating the intrinsic result. An isotherm that does not have this inherent problem is the virial adsorption isotherm:

$$p = \frac{q}{K_H} exp\left(A_1 q + A_2 q^2 + \cdots\right) \tag{8}$$

as there is no term involving θ included. On rearrangement, the plot of this isotherm becomes a straight line at low concentrations, provided only the first two terms of the series are retained:

$$ln\left(\frac{p}{q}\right) = -lnK_H + A_1 q \tag{9}$$

A plot of ln(p/q) versus q is a straight line of slope A_1 and intercept −ln(K_H). According to (Barrer 1978), the coefficient A_1 is slightly temperature dependent. The Henry's constant, K_H, may be expressed by the van't Hoff equation:

$$K_H = K_0 exp\left(\frac{-\Delta H_0}{RT}\right) \tag{10}$$

where K_0 is the pre-exponential factor and ($-\Delta H_0$) is the heat of adsorption at zero loading.

The Toth isotherm model, for energetic heterogeneous surfaces, is fitted to the fresh data that is reported in the supplementary data (Burgess 1989)

$$q = \frac{q_{max} p}{\left(b + p^t\right)^{1/t}} \tag{11}$$

In this model, K_H is (Valenzuela and Myers 1989)

$$K_H = q_{max} b^{-1/t} \tag{12}$$

The variation of the isosteric heat with loading may be found using the relationship from thermodynamics

$$q_{st} = -R\left(\frac{\partial \ln P}{\partial\left(\frac{1}{T}\right)}\right)_q \quad (13)$$

By plotting ln(p) versus 1/T at different fixed values of q, the variation of heat of adsorption with loading is determined.

3 Apparatus and procedure

The apparatus and procedure used in this study is identical to that reported in the earlier work of Abdul Rehman et al. (1990)

4 Results and discussion

The literature studies used for both zeolites are tabulated in Tables 4, 5. Five columns are displayed, year of publication, authors, zeolite source, % binder, and apparatus type. Studies in which the % binder is unknown were not considered further (Mulloth and Finn 1998; Merel et al. 2008; Tlili et al. 2009; Saha et al. 2010; Kyaw et al. 1997; Siriwardane et al. 2001; Li et al. 2009). As mentioned in the literature section, fresh data for adsorption of CO_2 on 13X zeolite, tabulated in Table 11 in supplementary data, and digitized or tabular data from the literature are used in this study.

The data for zeolite 5A are plotted as ln (q) versus ln(p), in Fig. 1a, and as q versus ln(p), in Fig. 1b, c. The saturation limit may be defined as the location on the isotherm where dq/dp tends to zero. This is generally the topmost point unless capillary condensation is observed. The isotherms which delineate the saturation point best are the log–log plots of the isotherms. Isotherms on log–log plots which have a slope of zero at their highest values are considered saturated and isotherms lacking this condition are considered unsaturated and are not included in the q_{max} calculation. Plots of q versus ln(p) assist in verifying the consistency of studies, i.e. verifying whether isotherms are crossing or are in the incorrect location or have wrong shape. Figure 1b illustrates the adsorption isotherms of carbon dioxide on zeolite 5A plotted as adsorbent concentration, q versus ln(p) that are retained after careful analysis. Removed isotherms are shown in Fig. 1c. The isotherms of (Pakseresht et al. 2002) and (Chen et al. 1990) have been removed due to not conforming to the shape or position of the retained isotherms. For (Pakseresht et al. 2002), the isotherm at 303 K appears to level off incorrectly, the isotherm at 373 K is out of position and convexing upward at the top end, and the isotherm at 573 K does not appear to be far enough to the right in comparison to the other isotherms. For (Chen et al. 1990) the isotherm at 298 K is out of position, adjacent to 398 K isotherms, and the 373 K isotherm is convexing upwards. Both sets of isotherms were measured in a volumetric apparatus. Low concentration isotherms were not included in the estimation of saturation q_{max} values as obviously they are far from saturation but they are included in the estimation of the intrinsic Henry constants. Examples are the isotherms of (Brandani 2003) and the 398, 423 and 443 K isotherm of Wang and LeVan (2009).

Table 4 CO_2 studies on 5A zeolite

5A				
Years	Authors	Adsorbent	Fraction Zeolite	Type
1990	Chen et al.	5A Union Carbide Co.	0.80	Volumetric
2002	Pakseresht et al.	5A Union Carbide Co.	0.80	Volumetric
1998	Mulloth and Finn	5A Allied Signal Inc.	Unknown	Volumetric
1998	Wang et al.	5A	1.0	Volumetric
2003	Brandani et al.	CaA	1.0	ZLC
2008	Merel et al.	5A Axens (IFP)	Unknown	Packed Bed
2009	Wang and Levan	5A Grace-Davison	0.80	Volumetric
2009	Tili et al.	5A	Unknown	Gravimetric
2010	Saha et al.	5A SINOPEC, China	Unknown	Volumetric

The data for the adsorption of carbon dioxide on 13X are plotted in Fig. 2a–c. Similar to the analysis for 5A, studies for 13X are plotted in two ways, as ln(q) versus ln(p) in Fig. 2a and as q versus ln(p) in Fig. 2b, to show the saturation limit and check for consistency respectively. After careful analysis the data at low concentration which consequently didn't reach saturation (Brandani 2003; Wang and LeVan 2009; Avgul 1968) are omitted from the analysis of the saturation loading, q_{max}. These are shown in Fig. 2b. Figure 2a shows the accepted data for the saturation loading study. Isotherms rejected for too low a concentration in the saturation study in Fig. 2b are included in the estimation of the intrinsic Henry constants.

As mentioned above, the saturation loading is taken as the value of q_{max} for the isotherms deemed close to saturation [indicated by leveling off] as shown in Figs. 1a and 2a. It is difficult to quantify the accuracy of this estimation as the approach to saturation is not clear in many cases. The estimated q_{max} values are deemed to be accurate to ± 3–5 %. The q_{max} values are plotted in Fig. 3a, b as q_{max} versus T_r for 5A and 13X respectively. Theoretical values derived from employing the modified Rackett's

Table 5 CO_2 studies on 13X zeolite

13X				
Years	Authors	Adsorbent	Fraction Zeolite	Type
1968	Avgul et al.	NaX-0.06H:0.94$NaAlO_2$:1.38SiO_2	1.0	Volumetric
1982	Hyun and Danner	Linde 13X pellets	0.8	Volumetric
1989	Burgess	Linde 13X pellets	0.8	Volumetric
1997	Kyaw et al.	13X Fuji-Davison	Unknown	Volumetric
1998	Wang et al.	13X	1.0	Volumetric
2001	Siriwardane et al.	Süd Chemie Inc	Unknown	Volumetric
2001	Pulin et al.	NaX	1.0	Gravimetric for < 100 kPa and Volumetric for > 100 kPa
2003	Cavenati et al.	13X CECA (France)	0.83	Gravimetric
2003	Brandani et al.	NaX	0.82	ZLC
2008	Merel et al.	13X Axens (IFP)	Unknown	Packed Bed
2009	Li et al.	13X pellets	Unknown	Gravimetric
2009	Wang and Levan	13X Grace-Davison	0.80	Volumetric

equation are calculated using Eq. 5 and are shown as the dashed lines in Fig. 3a, b. The value of ε_z and ρ_z are taken from Table 3 data and are 0.387 and 1.48 for 5A and 0.455 and 1.43 for NaX respectively. Figure 3a, b indicate a good agreement between the modified Rackett equation and the experimental values in the subcritical region below $T_r = 0.9$, but at values above this value and in the supercritical region the deviation increases with the increase of temperature.

For NaX(13X) a dichotomy is observed in the data for q_{max} which is not observed in the 5A data. The data by (Pulin 2001) and (Cavenati et al. 2004) for 13X in Fig. 3b is significantly higher than other studies. Pulin (2001) measured the carbon dioxide adsorption between 0.45 and 5.4 MPa and observed an expansion of the zeolite under these conditions attributing the high loading to this expansion. The data by (Pulin 2001) is trending similar to other studies for increasing reduced temperature whereas the data of (Cavenati et al. 2004), decreases much more sharply with T_r than for all other studies The remaining studies of (Avgul 1968; Barrer and Gibbons 1965; Burgess 1989; Hyun 1982; Wang and LeVan 2009) do not support the results of (Pulin 2001) or (Cavenati et al. 2004) having significantly lower q_{max} values. Further, the lower studies are in good agreement with the theoretical results of the calculation of q_{max} using Eq. 5 using Rackett's equation for density up to a reduced temperature of $T_r = 0.9$. Above a T_r of 0.9, the q_{max} values are slightly above the theoretical value suggesting that the molar volumes of CO_2 are smaller in the zeolite than in the liquid phase (Huang et al. 2005). Further many of the values are above a T_r of 1 for which we have no theoretical equation for predictive purposes. The saturation loading appears to change linearly with temperature above a T_r of 0.9 up to a T_r of 1.25. To evaluate this observation the values of q_{max} for a T_r range of $0.9 \leq T_r \leq 1.25$ are linearly regressed:

$$For\ 5A\ zeolite: \quad q_{max} = -34.291T_r + 55.696: \quad 0.9 \leq Tr \leq 1.25: \quad R = 0.984 \tag{14}$$

$$For\ 13X\ zeolite: \quad q_{max} = -32.866T_r + 55.078: \quad 0.9 \leq T_r \leq 1.25: \quad R = 0.869 \tag{15}$$

A summary of saturation loading, experimental and theoretically calculated using Eq. 5 is presented in Table 6.

The q_{max} data in Fig. 3a, b for the region $0.9 < T_r < 1.0$ are the sole data observed by the authors to be greater than the q_{max} value derived using Eq. 5. In all other studies, the q_{max} data is observed to be below the value estimated by Eq. 5 up to the critical adsorbate reduced temperature for both 5A and 13X zeolite (Loughlin and Abouelnasr 2009) and (Al-Mousa et al. 2011). Abouelnasr (2011, Personal Communication) has suggested that the T_r value of 0.9 may be the critical adsorbate reduced temperature and this may be the reason why both linear regressed plots originate at a T_r of 0.9 up to a T_r of 1.25. The linear decrease represents a significant different behavior for the CO_2 molecule from the *n* alkanes in 5A zeolite as there is no leveling off of the loading above the critical adsorbate reduced temperature as was observed for the n alkanes on 5A zeolite. However, the higher experimental q_{max} values indicate either a smaller partial molar volume for the adsorbed CO_2 molecule than is observed in the saturated liquid phase (Huang et al. 2005) or a significant expansion of the NaX zeolite as observed by (Pulin 2001). The partial molar volumes of CO_2 are shown calculated for the saturated liquid phase and for the adsorbed phase in Table 7. Also shown is the partial molar volume at $T_r = 1.046$ in the bulk phase and in an ionic liquid for comparison purposes. The partial molar

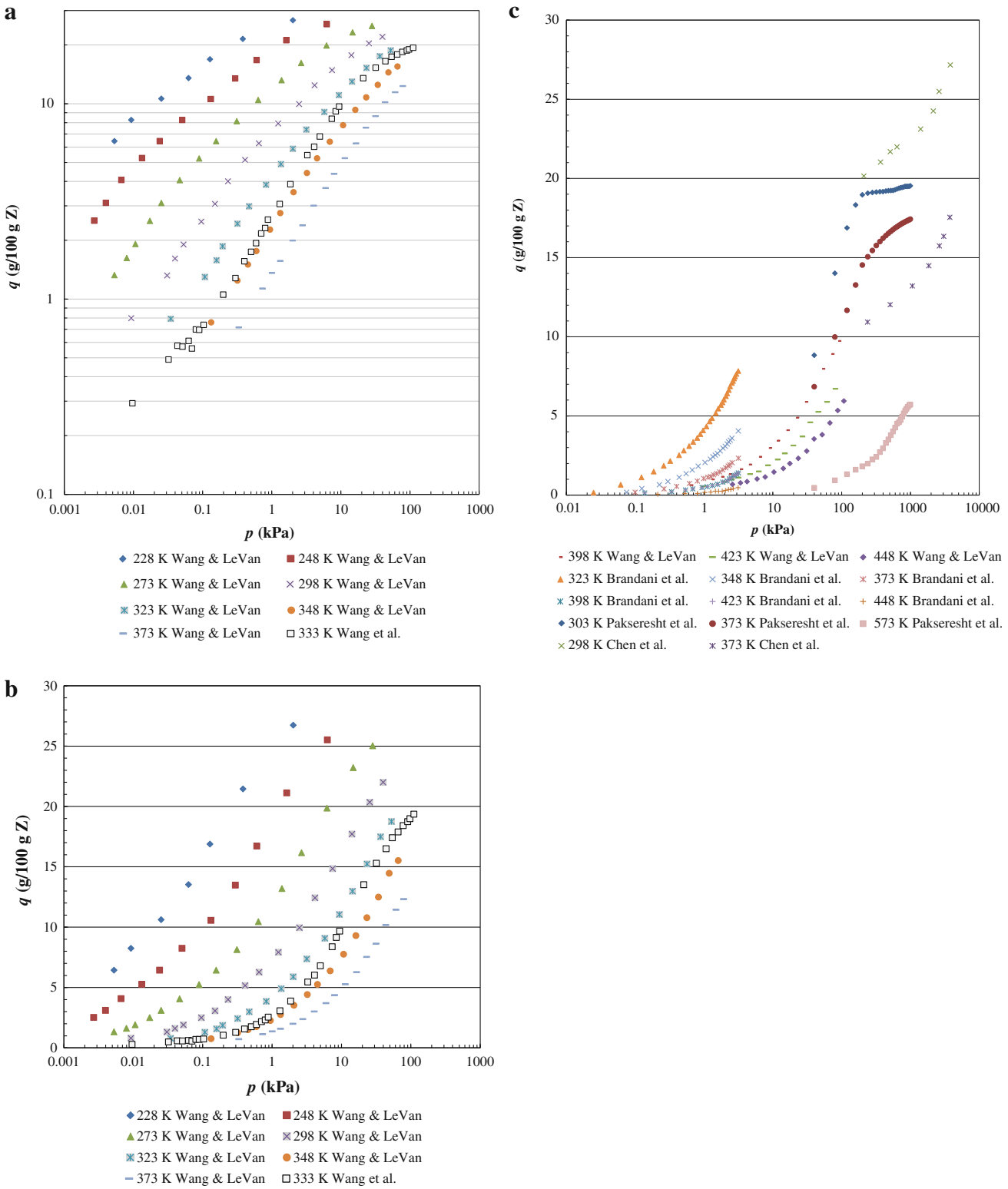

Fig. 1 **a** ln(q) versus ln(p) on zeolite 5A for different studies showing only considered data for saturation loading estimation. **b** q versus ln(p) on zeolite 5A for different studies showing only considered data for saturation loading estimation. **c** q versus ln(p) on zeolite 5A for different studies showing eliminated data for saturation loading estimation

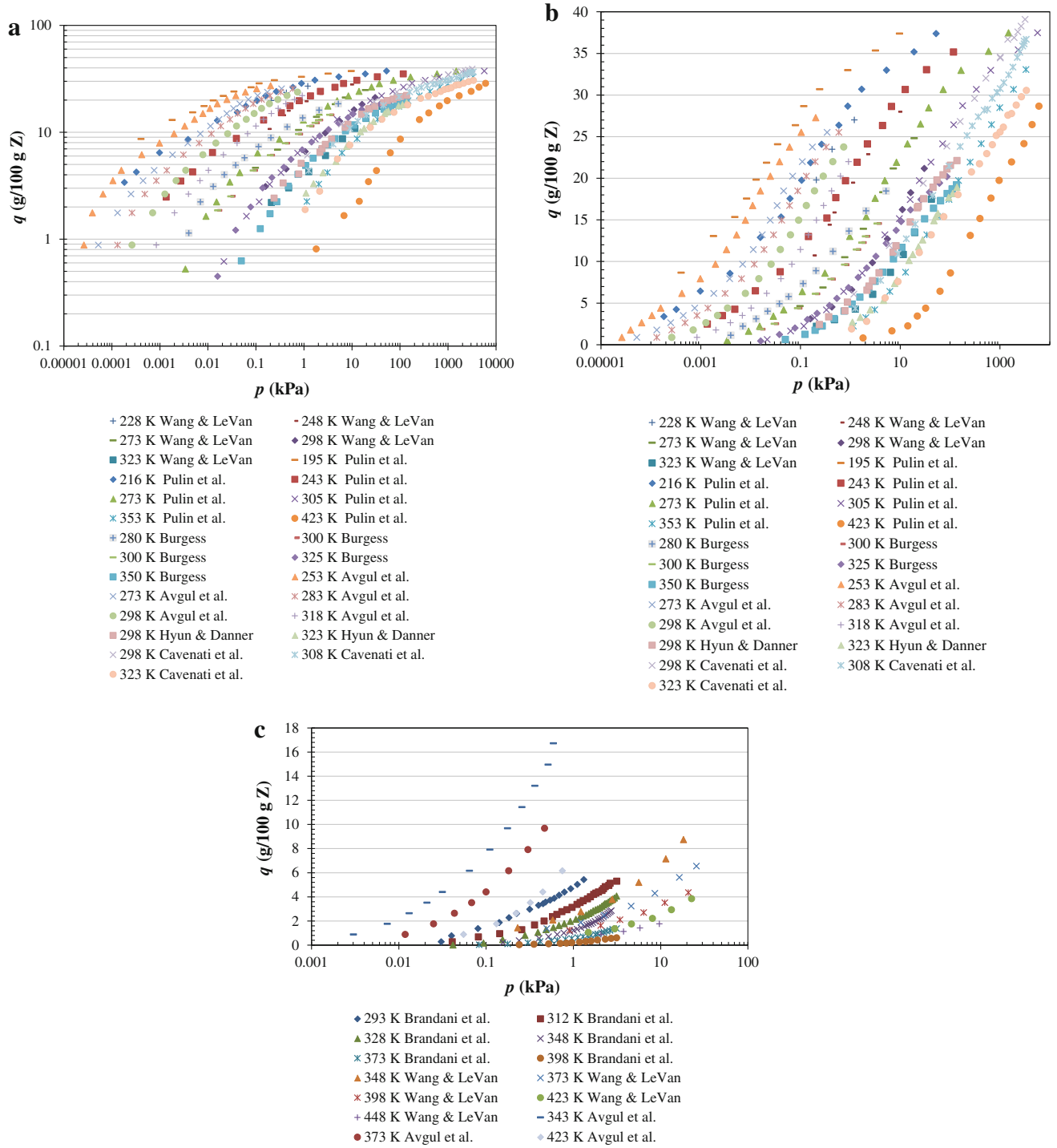

Fig. 2 **a** ln(q) versus ln(p) on zeolite 13X for different studies showing only considered data for saturation loading estimation. **b** q versus ln(p) on zeolite 13X for different studies showing low concentration loading

volumes of the adsorbed phase are 5–25 % less than for the saturated liquid. At the vapor liquid critical point, the adsorbed molar volume is one half that of the saturated critical phase. This latter value is similar to what is observed in ionic liquids as the value at $T_r = 1.046$ is half that of the equivalent value in the bulk phase. It is clear that the partial molar volumes of the adsorbed phase are less than that of an equivalent saturated liquid, and that this is similar to results observed in the carbon dioxide ionic liquid system. We can conclude that q_{max} can satisfactorily be calculated using Eq. 5 up to a reduced temperature of 0.9 and using Eqs. 14 and 15 above this T_r for the CO_2-5A

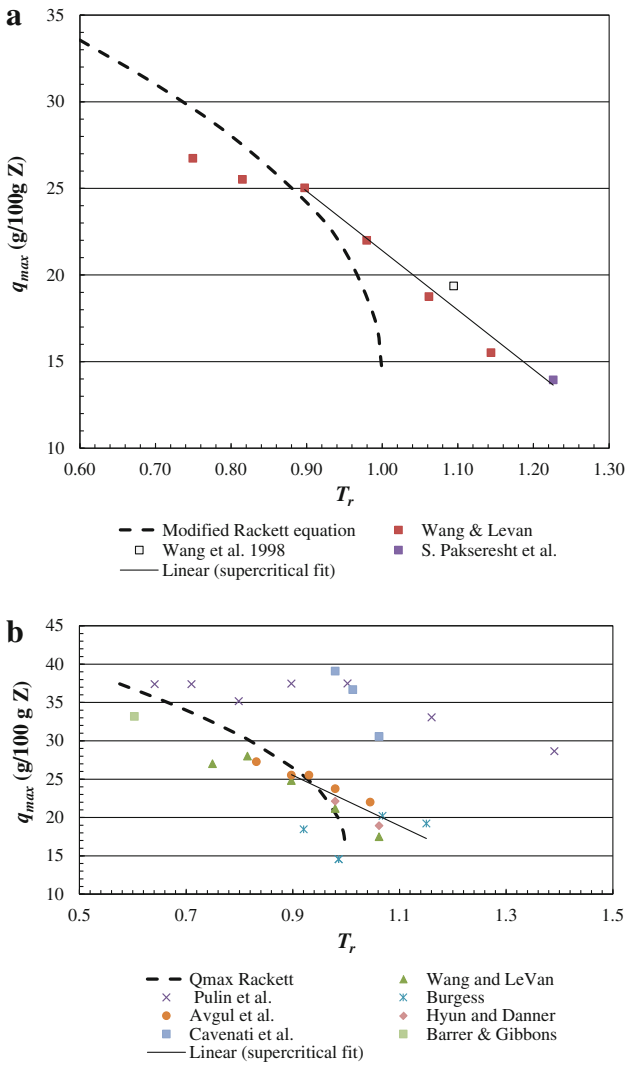

Fig. 3 **a** Plot of values of the saturation loading from the Modified Rackett equation, q_{max}, and the corresponding values from experimental data for zeolite 5A. **b** Plot of values of the saturation loading from the Modified Rackett equation, q_{max}, and the corresponding values from experimental data for zeolite 13X

and CO_2-13X systems. More experimental data is required above a T_r of 1.25.

To determine the intrinsic Henry constants, Eq. 9, is plotted in Fig. 4a, b as a plot of ln(p/q) versus q in the low loading region, where $q \leq 7$. This plot yields a straight line for each isotherm and is strongly linear for both systems up to 7 g/100 g Z. Some outliers and isotherms with insufficient points in the low region were omitted. The Henry constant values are calculated from the intercept of the straight lines in Fig. 4a, b, and are summarized in Table 8. The K_H values are plotted in a van't Hoff plot as shown in Fig. 5a, b, and the regressed van't

Table 6 A summary of values of the saturation loading from the modified Rackett equation, q_{max}/(g/100 g Z), and the corresponding values from experimental data for 5A and 13X

Experimental data			Modified Rackett equation	
T_r	Reference	q_{max} (g/100 g Z)	T_r	q_{max} (g/100 g Z)
5A zeolite				
0.75	Wang and Levan	26.73	0.75	29.6
0.82	Wang and Levan	25.52	0.82	27.52
0.9	Wang and Levan	25.03	0.9	24.3
0.98	Wang and Levan	22	0.98	18.91
0.98	Saha et al.	22.27	0.98	18.91
1.06	Wang and Levan	18.76	1.06	19.29[a]
1.09	Wang et al.	19.36	1.09	18.16[a]
1.14	Wang and Levan	15.51	1.14	16.47[a]
1.23	S. Paksereshet et al.	13.94	1.23	13.65[a]
13X Zeolite				
0.6	Barrer & Gibbons	33.18	0.6	33.49
0.64	Pulin et al.	37.39	0.64	32.55
0.71	Pulin et al.	37.39	0.71	30.73
0.75	Wang and LeVan	27.01	0.75	29.6
0.8	Pulin et al.	35.16	0.8	28.07
0.82	Wang and LeVan	28	0.82	27.52
0.83	Avgul et al.	27.28	0.83	26.95
0.9	Wang and LeVan	24.81	0.9	24.3
0.9	Pulin et al.	37.46	0.9	24.3
0.9	Avgul et al.	25.52	0.9	24.3
0.92	Burgess	18.46	0.92	23.18
0.93	Avgul et al.	25.52	0.93	22.64
0.98	Wang and LeVan	21.18	0.98	18.91
0.98	Avgul et al.	23.76	0.98	18.91
0.98	Hyun and Danner	22.11	0.98	18.91
0.98	Cavenati et al.	39.08	0.98	18.91
0.99	Burgess	14.56	0.99	18.08
0.99	Burgess	14.56	0.99	18.08
1	Pulin et al.	37.47	1	No Prediction
1.01	Cavenati et al.	36.68	1.01	No Prediction
1.05	Avgul et al.	22	1.05	20.72[b]
1.06	Wang and LeVan	17.49	1.06	20.18[b]
1.06	Hyun and Danner	18.92	1.06	20.18[b]
1.06	Cavenati et al.	30.55	1.06	No Prediction
1.07	Burgess	20.2	1.07	19.96[b]
1.15	Burgess	19.21	1.15	17.26[b]
1.16	Pulin et al.	33.06	1.16	No Prediction
1.39	Pulin et al.	28.65	1.39	No Prediction

[a] Calculated using Eq. 14

[b] Calculated using Eq. 15

Table 7 Partial molar volumes of carbon dioxide in cm^3/mol

Adsorbate-adsorbent system		
T_r	V_{sat} liquid	V adsorbed phase
0.8	40.92	40.92
0.85	43.56	38.28
0.9	47.52	40.92
0.95	53.68	43.868
1.0	93.28	46.64
Bulk phase and ionic liquid		
1.046 (at 318.15 K & 200 bar)	55	29

Hoff values are presented in Eqs. 16 and 17. The slope of the straight line is the enthalpy of adsorption ($-\Delta H_0$). This was calculated to be 44.15 for the five studies used in the CO_2-5A system and 51.34 for the seven studies used in the CO_2-13X system. These values are higher than the values of 38.4, 40.4 [CaA], 32.8 [5A] and 40.6 for NaX reported by Brandani et al. (2003). The correlation coefficient for the van't Hoff plots is 0.999 for the CO_2-5A system, and 0.899 for the CO_2-13X system. The correlation coefficient of 0.999 is a staggering number for studies from five different laboratories for the CO_2-5A system. The lower correlation for the NaX system may be due to small imperceptible impurities between the different laboratories. For NaX, the data of Avgul et al. (1968) is shown plotted in Fig. 4b. However, it is not included in the calculation of the Henry constant or the heat of adsorption for the CO_2-13X system. The reason for this is that the NaX zeolite used by Avgul et al. had the formula weight of $0.06H:0.94NaAlO_2:1.38SiO_2$ and the presence of the hydrogen atom appears to alter the adsorption forces significantly. The inclusion of the hydrogen in the formula gave Henry constants two orders of magnitude greater than for the was omitted from the calculation. The inclusion of hydrogen in the formula weight did not affect the saturation values, and that is why the data of Avgul et al. was retained in the q_{max} study.

$$For\ 5A\ zeolite: \quad K_H = 8.550 * 10^{-7} \exp\left(-\frac{44.15}{RT}\right): \quad 248\mathrm{K} < T < 423K: \quad R = 0.999 \tag{16}$$

$$For\ 13X\ zeolite: \quad K_H = 2.506 * 10^{-5} \exp\left(-\frac{51.34}{RT}\right): \quad 253\mathrm{K} < T < 448K: \quad R = 0.899 \tag{17}$$

In calculating the Henry constants using the data in Fig. 4a, b, the authors removed outliers. However, some outliers became too consistent to be ignored. The removed outliers are shown in Fig. 6 in a plot of ln(p/q) versus q at

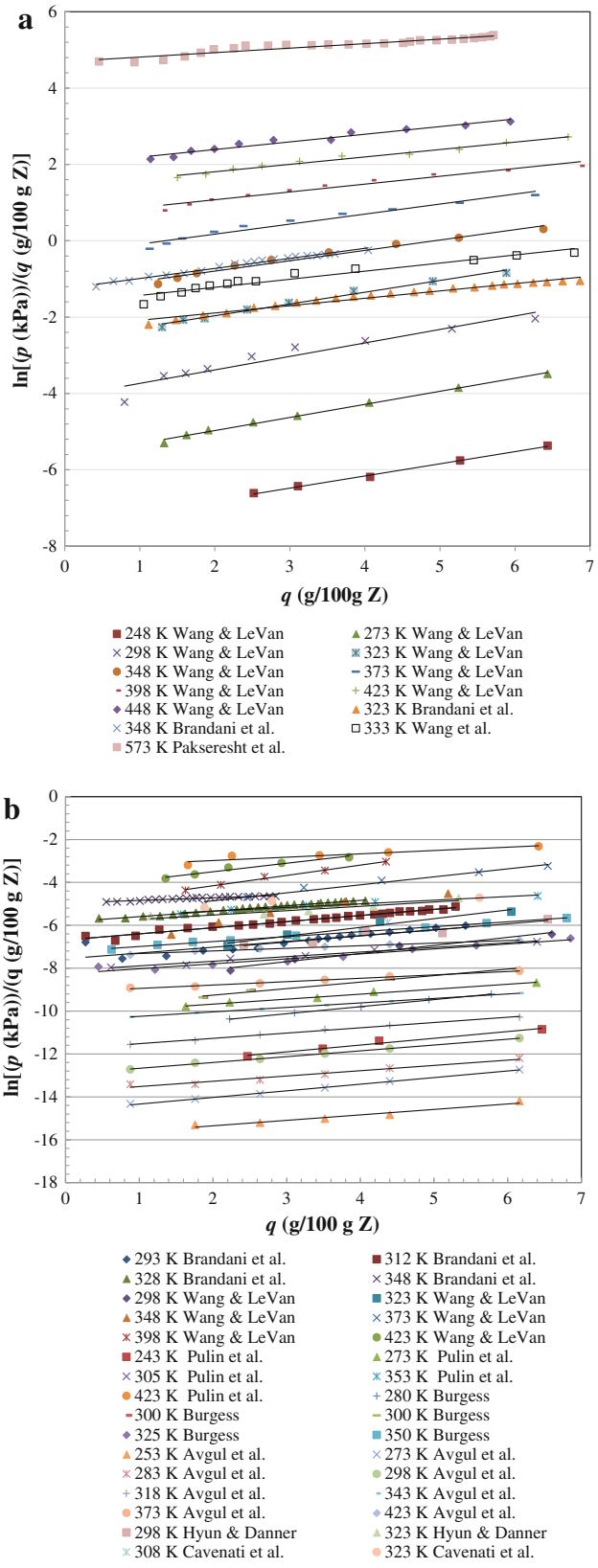

Fig. 4 **a** plot of ln[(*p*/kPa)/(*q*/(g/100 g Z)] versus *q*/(g/100 g Z) without outliers at low loading region, i.e. *q*/(g/100 g Z) ≤ 7 for zeolite 5A. **b** Plot of ln(*p*/*q*) versus *q* without outliers at low loading region, i.e. *q*/(g/100 g Z) ≤ 7 for zeolite 13X

Table 8 Summary of Henry constants for CO_2 studies on 5A and 13X zeolite

5A			13X		
Reference	T/K	K_H/(g/100 g Z kPa)	Reference	T/K	K_H/(g/100 g Z kPa)
Wang and Levan	247	1094.00	Avgul et al.	253	7.69E + 06
	273	286.40		273	2.28E + 06
	298	48.72	Pulin et al.	273	2.53E + 04
	323	13.22	Burgess	280	6.66E + 04
Brandani et al.	323	9.76	Avgul et al.	283	1.11E + 06
Wang et al.	333	5.17	Wang and Levan	298	6807.34
Wang and Levan	348	3.80	Hyun & Danner	298	2068.27
Brandani et al.	348	3.49	Avgul et al.	298	4.16E + 05
Wang and Levan	373	1.42	Burgess	300	1.69E + 04
	398	0.52		300	1.689E + 04
	423	0.24	Pulin et al.	305	3318.78
	448	0.14	Brandani et al.	312	828.76
Pakseresht et al.	573	0.0091	Avgul et al.	318	1.29E + 05
			Wang and Levan	323	2252.87
			Hyun & Danner	323	373.76
			Burgess	325	4484.21
			Brandani et al.	328	346.61
			Avgul et al.	343	3.48E + 04
			Brandani et al.	348	148.11
			Wang and Levan	348	790.09
			Burgess	350	1364.02
			Pulin et al.	353	384.33
			Brandani et al.	373	71.79
			Wang and Levan	373	271.96
			Avgul et al.	373	8291.94
			Wang and Levan	398	167.51
			Brandani et al.	398	20.25
			Wang and Levan	423	66.09
			Pulin et al.	423	26.84
			Avgul et al.	423	1693.62
			Wang and Levan	448	93.53

Note the data of Avgul et al. is for NaX [0.06H:0.94$NaAlO_2$:1.38SiO_2] rather than NaX

an extremely low loading, $\leq$1 for 13X. It is clear that there is an unusual kink upwards at $q < 0.5$ indicating that an unusual thermodynamic effect has occurred. The reason for these outliers can be attributed to a differing kind of bonding for the initial single molecule of carbon dioxide adsorption. Llano-Restrepo postulates that CO_2 molecules interacts with either one Na(2) ion to form a Na^+-CO_2 complex or with one Na(3) ion to form either a partially ionized or a bidentate carbonate species (Llano-Restrepo 2010). It is possible that either of these complexations could result in the initial unusual observed effect. Further, these complexations could cause the calorimetric measurement of the heat of adsorption to be larger initially as has been reported by Dunne et al. (1996) and Shen et al. (2000). Also, since it only occurs at loadings of less than 0.5 g/100 g Z, it is quite possible that most of the non-calorimetric studies miss this effect as has been reported by Shen et al.

The isosteric heats were calculated using Eq. 13 by plotting ln(p) versus 1,000/T at constant loading as shown in Fig. 7a, b for the 5A and 13X zeolites respectively. Five studies were used for the 5A calculations and seven studies were used for the 13X calculations. From Eq. 13, the slopes of the straight lines in the Figures are the isosteric heats at the respective loading. The isosteric heats are plotted in Fig. 8a as functions of loading. The isosteric heat for 5A is slightly greater than that for 13X probably due the adsorption field in the more confined cavity. The isosteric

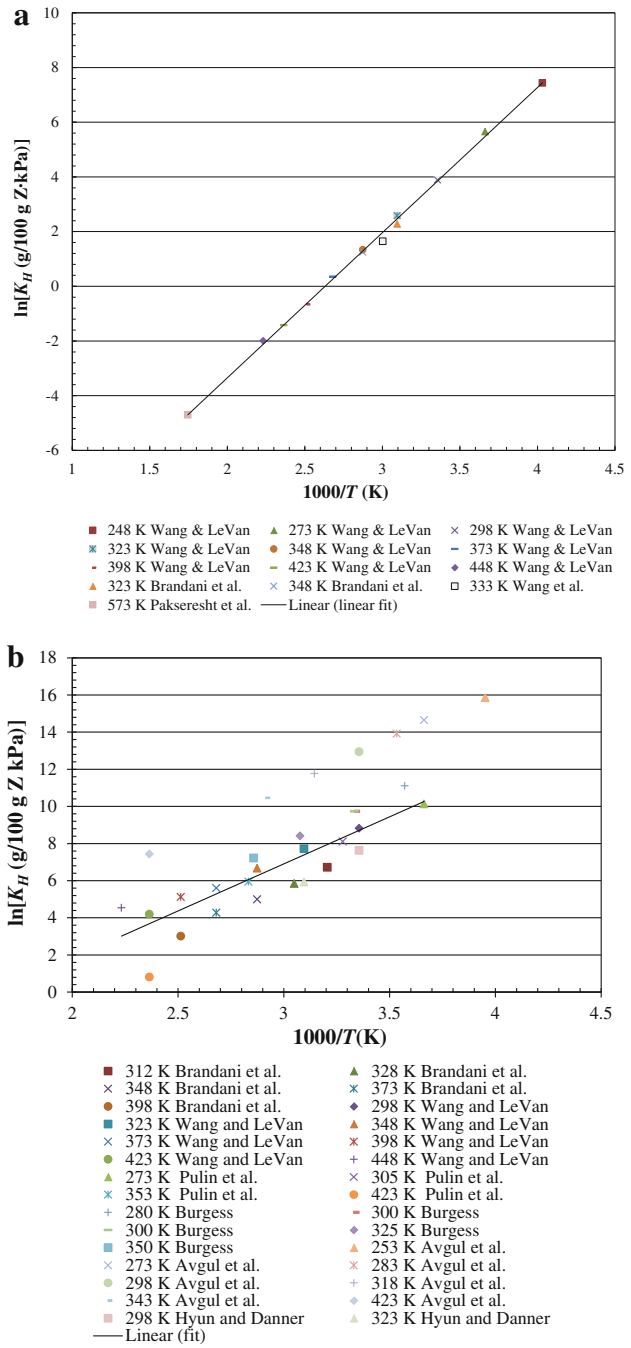

Fig. 5 **a** van't Hoff plot for zeolite 5A. **b** van't Hoff plot for zeolite 13X excluding Avgul et al.'s values

heat decreases from approximately 45 kJ/mol at zero loading, decreasing linearly initially to ~35 kJ/mol, plateauing in the mid region $0.4 \leq \theta \leq 0.6$, and decreasing to 25.2 kJ/mol as saturation is approached. The heat of sublimation of carbon dioxide is 25.2 kJ/mol which is the lowest isosteric heat observed. The isosteric heats at different loadings for zeolite 5A and 13X are summarized in

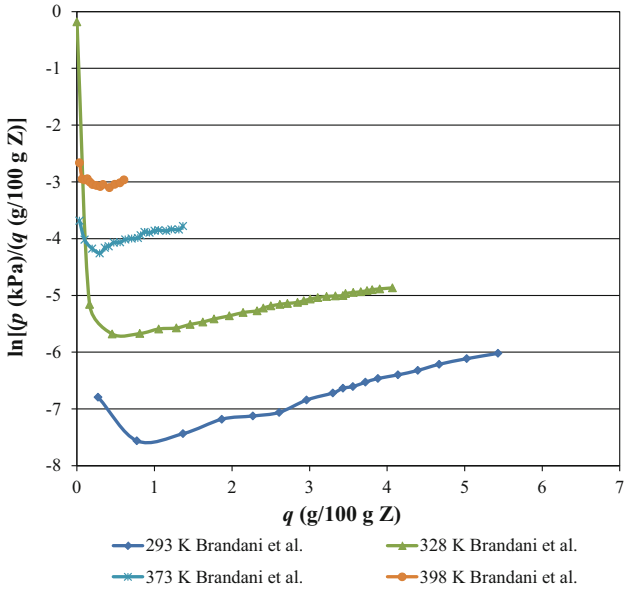

Fig. 6 Plot of ln(p/q) versus q without outliers at low loading region, i.e. $q \leq 7$ for zeolite 13X showing isotherms with outliers

Table 9. The value of 45 kJ/mol is similar to the value of 44.1 kJ/mol obtained in the van't Hoff plot at zero loading for the Henry constant for 5A zeolite but is less than the value of 51.3 kJ/mol obtained for 13X zeolite in a similar van't Hoff plot.

The data for 13X is again plotted in Fig. 8b together with the study of Dunne et al.[30] and the two studies of Shen et al., one adsorption isosteres and one calorimetric measurements. Further studies are available in Fig. 5 of Llano-Restrepo but have not been included as the figure becomes congested. The two calorimetric studies of Dunne et al. and Shen and Bulow have a zero loading value of ~50 kJ/mol, and a gradually decreasing region to a plateau of ~36 kJ/mol in the middle region; Dunne et al.'s study subsequently decreases as it starts to approach the heat of sublimation at higher loadings. The reported values in this study are lower than the calorimetric values in the decreasing region, similar in the plateau region, and in the approach to saturation region. The isosteric heat curve reported by Shen and Bulow is the lowest of all the studies by ~3 to 5 kJ/mol. The zero calorimetric loading is consistent with the value of 51.3 kJ/mol obtained in the van't Hoff study of the Henry constant determination. The consistently lower values of the isosteric heat determination from the calorimetric measurements reported in the literature may be attributed to the outlier region of <0.5 (g/100 g Z) reported in Fig. 6 above. Finally, the sharp decrease from 50 kJ/mol to the plateau region at 36 kJ/mol may be attributed to the interaction of the Na^+ ion with the quadrupole moment of CO_2; at high

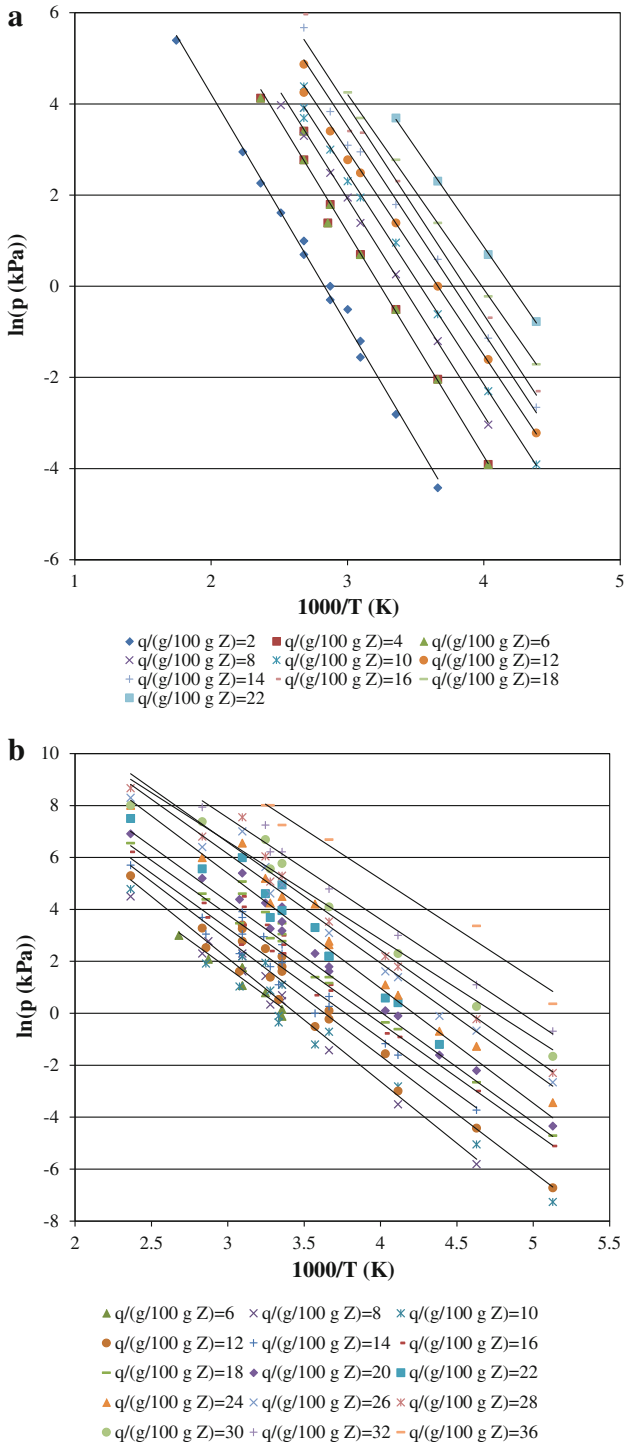

Fig. 7 **a** Plot of ln(p) versus 1,000/T at various loadings for zeolite 5A. **b** Plot of ln(p) versus 1,000/T at various loadings for zeolite 13X

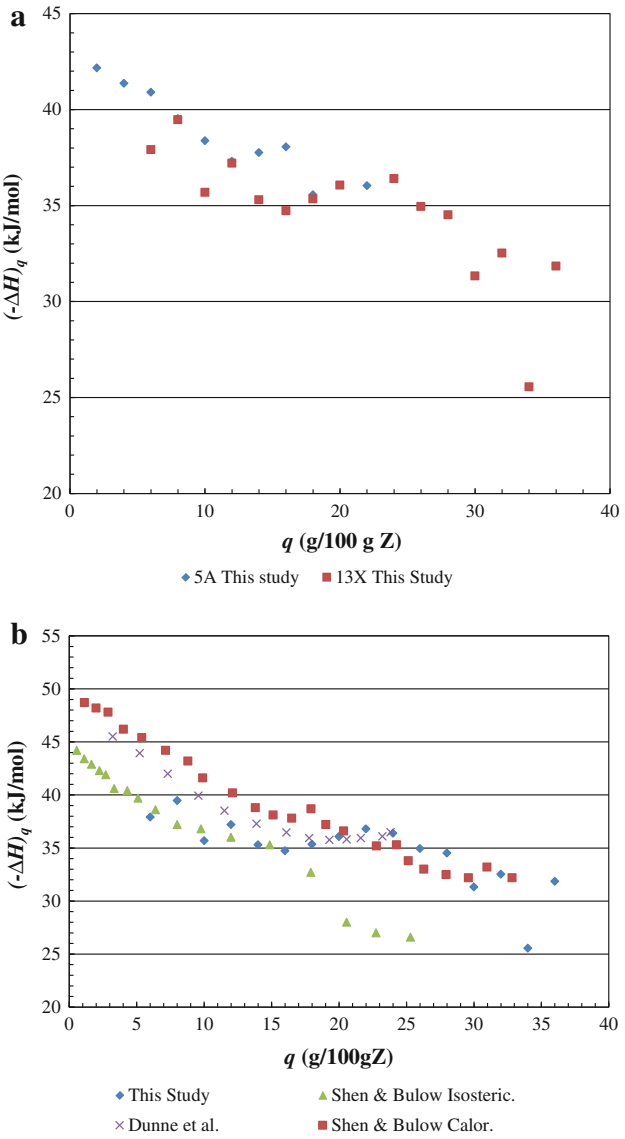

Fig. 8 **a** Isosteric heats as functions of loading for zeolites 5A and 13X. **b** Isosteric heats as functions of loading for zeolite 13X for different studies. Isosteric heats as functions of loading for zeolite 13X for different studies

coverage the high energy Na^+ ions become saturated and the gas–solid interaction energy is mainly dispersion.

Fresh data for the adsorption of CO_2 on zeolite 13X by Burgess is presented in Table 11 (in supplementary material) and fitted to Toth isotherm, Eq. 11 (Burgess 1989). The Toth parameters are tabulated in Table 10 with the correlation coefficient (all >0.99) for the Toth fit. So the Toth model fits the data excellently.

The values of q_{max} and K_H obtained from the Toth model is compared with the intrinsic values obtained from the previous analysis, where the value of q_{max} is derived directly from the Toth model or Eq. 15 and the Henry constant is derived by Eq. 12 and from the virial isotherm, Eq. 9. Clearly, there is a large difference between the q_{max} values; further the trending of q_{max} with T_r is opposite to that expected, increasing with T_r for the Toth isotherm, and decreasing with T_r for the intrinsic values. Similarly, there is a large difference between the values of K_H between the

Toth and virial isotherms. There is a twofold reason for this difference: firstly, the fit is only for a small range of T_r and secondly, the value of K_H is impacted by the value of q_{max}, as they interact in the model. The Toth model's K_H values are lower than the values obtained earlier and summarized in Table 9. The true K_H values can only be obtained from a virial plot. This comparison indicates the difficulty of deriving intrinsic parameters from model isotherms due to parameter interaction.

Finally, the fact that the zeolites 5A and 13X may not have perfect crystal forms and/or may have different zeolite formulas depending on the different Si/Al ratios needs to be considered. The parameter q_{max} appears to be unaffected by either of these possibilities. For 13X there may be some difference depending on the Angtrom variation of the width of the cubic crystal lattice. The authors were not able to detect this; a precise systematic study for different crystal lattices at high loadings is probably required to determine if a variation exists. The biggest variation arises in the establishment of the K_H values. For 5A this appears to be limited as may be observed in Fig. 5a where the van't Hoff fit is excellent (correlation coefficient 0.999). For 13X there is a large variation as may be observed in Fig. 5b (correlation coefficient 0.899. The data of Avgul et al. is omitted from the correlation due to the presence of the hydrogen ion in the formula weight). The data shows a significant scatter probably indicative of different ionic species in the various formula weights.

Table 9 Isosteric heats $(-\Delta H)_q$ at different loadings q for 5A and 13 X

5A		13X	
q/(g/100 g Z)	$(-\Delta H)_q$/(kJ/mol)	q/(g/100 g Z)	$(-\Delta H)_q$/(kJ/mol)
2	42.17	2	28.00
4	41.37	4	23.93
6	40.90	6	37.91
8	39.53	8	39.47
10	38.38	10	35.69
12	37.30	12	37.21
14	37.76	14	35.30
16	38.06	16	34.73
18	35.56	18	35.35
20	31.09	20	36.07
22	36.04	22	36.80
		24	36.40
		26	34.95
		28	34.52
		30	31.33
		32	32.52
		34	25.56
		36	31.85

5 Conclusions

In this study, three intrinsic properties, q_{max}, the saturation loading, K_H the Henry constant and $(-\Delta H)_q$, the isosteric heat of sorption are derived from literature studies and fresh data. Provided T_r is <0.9, the intrinsic q_{max} values agree with values estimated from crystallographic properties and the saturated density calculated using the Rackett equation. Above T_r of 0.9, the molecular volume of adsorbed CO_2 is less than the molecular volume of the equivalent saturated liquid giving q_{max} values greater than those predicted from Eq. 5. A regressed fit is applied to the data for q_{max} in the region $0.9 \leq T_r \leq 1.25$.

The intrinsic Henry constants were surprisingly consistent for 5A (R = 0.999 for 5 different laboratories) but not as consistent for 13X (R = 0.899 for 7 different laboratories). The heat of adsorption values determined at zero loading by the van't Hoff plot were in agreement with the values reported for the isosteric heats of adsorption.

The isosteric heats started at zero loading at 45(isosteric) to 50 kJ/mol(calorimetric), decreased linearly to a plateau region of 36 kJ/mol in the region $0.4 \leq \theta \leq 0.6$, before

Table 10 Toth parameters for Burgess's data

T_r	q_{max}/(g/100 g Z)	q_{max} (Rackett)	R	b/(1/kPa)	t	K_H/(g/100 g Z kPa) (Toth)	K_H/(g/100 g Z kPa) (virial)
0.92	18.4580	23.18	0.9989	0.2771	0.348	1141	6.66E+04
0.99	20.8560	18.08	0.9998	0.4209	0.2640	1058	1.69E + 04
0.99	22.2860	18.08	0.9998	0.4197	0.421	1038	1.689E+04
1.07	23.3068	19.96[a]	0.9985	0.7063	0.458	50	4484.21
1.15	23.8480	17.26[a]	0.9999	1.0586	0.417	22	1364.02

[a] Calculated using Eq. 15

subsequently falling to 25.2 kJ/mol, the sublimation value, as saturation is approached.

Acknowledgments The authors wish to acknowledge the support of the American University of Sharjah during the execution of this study. The authors also wish to acknowledge Alexander Burgess for the data measurements of CO_2 on Linde 13X zeolite. Also, this paper was presented at the Fall 2011 meeting of AIChE in Minneapolis. Finally, the authors wish to acknowledge an unnamed reviewer for the observations raised in the last paragraph of the paper.

References

Abdul-Rehman, H.A., Hasanain, M.A., Loughlin, K.F.: Quaternary, ternary, binary and pure component sorption on zeolites. 1. Light alkanes on Linde S-115 silicalite at moderate to high pressures. Ind. Eng. Chem. Res. **29**, 1525–1535 (1990)

Al-Mousa A.A., Abouelnasr D., Loughlin K.F.: Review and analysis of saturation loadings for subcritical alkane adsorption on 13X zeolite. In: Presented in session: experimental Methods in Adsorption, Fall 2011, AIChE (2011)

Avgul N.N., Aristov B.G., Kiselev A.V., Ya L.: Heat of Adsorption of carbon dioxide by NaX and NaA zeolites and dependence of the adsorption on gas pressure and temperature. Russ. J. Phys. Chem. **42**(10), 2678–2682 (1968)

Barrer, R.M., Gibbons, R.M.: Zeolite carbon dioxide: energetics and equilibria in relation to exchangeable cations in faujasite. J. Chem. Soc. Farad. Trans. **61**, 941–961 (1965)

Barrer, R.M.: Zeolites and Clay Minerals. Academic, London (1978)

Brandani, F., Ruthven, D.M., Coe, C.G.: Measurement of adsorption equilibrium by the zero length column (ZLC) technique. Part 1: single component systems. Ind. Eng. Chem. Res. **42**, 1451–1461 (2003)

Breck, D.W.: Zeolite Molecular Sieves. Wiley, New York (1974)

Burgess, A.: Computer modeling of equilibrium adsorption isotherms: CO_2 on 13X zeolite. Senior Design Project, King Fahd University of Petroleum & Minerals, Dhahran (1989)

Cavenati, S., Grande, C.A., Rodrigues, A.E.: Adsorption equilibrium of methane, carbon dioxide, and nitrogen on zeolite 13X at high pressures. J. Chem. Eng. Data **49**, 1095–1101 (2004)

Chen, Y.D., Ritter, J.A., Yang, R.T.: Nonideal adsorption from multicomponent gas mixtures at elevated pressures on a 5A molecular sieve. Chem. Eng. Sci. **45**, 2877–2894 (1990)

Dubinin, M.M., Astakhov, V.A.: Development of theories on the volume filling of microporous adsorbents. 2. General fundamentals of the theory of gas and vapor adsorption on zeolites. Izvestiya Akademii Nauk SSSR. Seriya Khimicheska **1**, 11–17 (1971)

Dunne, J.A., Rao, M., Sircar, S., Gorte, R.J., Myers, A.L.: Calorimetric heats of adsorption and adsorption isotherms. 2 O2, N2, Ar, CO2, CH4 and SF6 on NaX, H-ZSM-5 and Na-ZSM-5 zeolites. Langmuir **12**, 5896–5904 (1996)

Huang, X., Margulis, C.J., Li, Y., Berne, B.J.: Why is the partial molar volume of CO_2 so small when dissolved in a room temperature ionic liquid? Structure and dynamics of CO_2 dissolved in [Bmim +][PF6]. J. Am. Chem. Soc. **127**, 17842–17851 (2005)

Hyun, S.H., Danner, R.P.: Equilibrium adsorption of ethane, ethylene, isobutane, carbon dioxide and their binary mixtures. J. Chem. Eng. Data **27**, 196–200 (1982)

Kyaw, K., Shibata, T., Watanabe, F., Matsuda, H., Hasatani, M.: Applicability of zeolite for CO_2 storage in a CaO–CO_2 high temperature energy storage system. Energy Convers. Manag. **38**, 1025–1033 (1997)

Li, G., Xiao, P., Webley, P.A., Zhang, J., Singh, R.: Competition of CO_2/H_2O in adsorption based CO_2 capture. Energy Procedia **1**, 1123–1130 (2009)

Llano-Restrepo, M.: Accurate correlation, structural interpretation and thermochemistry of equilibrium adsorption isotherms of carbon dioxide in zeolite NaX by means of the GSTA model. Fluid Phase Equilib. **293**, 225–236 (2010)

Loughlin, K.F., Abouelnasr, D.M.: Sorbate densities on 5A zeolite above and below the critical conditions. Adsorption **15**, 521–533 (2009)

Merel, J., Clausse, M., Meunier, F.: Experimental investigation on CO_2 post-combustion capture by indirect thermal swing adsorption using 13X and 5A zeolites. Ind. Eng. Chem. Res. **47**, 209–215 (2008)

Mulloth, L.M., Finn, J.E.: Carbon dioxide adsorption on a 5A zeolite designed for CO_2 removal in spacecraft cabins. NASA/TM (1998)

Pakseresht, S., Kazemeini, M., Akbarnejad, M.M.: Equilibrium isotherms for CO, CO_2, CH_4, and C_2H_4 on the 5A molecular sieve by a simple volumetric apparatus. Sep. Purif. Technol. **28**, 53–60 (2002)

Pulin, A.L., Fomkin, A.A., Sinitsyn, V.A., Pribylov, A.A.: Adsorption and adsorption induced deformation of NaX zeolite under high pressure of carbon dioxide. Russ. Chem. Bull. **50**, 60–62 (2001)

Saha, D., Bao, Z., Jia, F., Deng, S.: Adsorption of CO_2, CH_4, N_2O, and N2 on MOF-5, MOF-177, and zeolite 5A. Environ. Sci. Technol. **44**, 1820–1826 (2009)

Saha, D., Bao, Z., Jia, F., Deng, S.: Adsorption of CO2, CH4, N20, and N2 on MOF-4, MOF-177, and zeolites 5A. Environ. Sci. Technol. **44**, 1820–1826 (2010)

Shen, D., Bulow, M.: Isosteric study of sorption thermodynamics of single gases and multicomponent mixtures on microporous materials. Microporous Mesoporous Mater. **22**, 237–249 (1998)

Shen, D., Bulow, M., Siperstein, F., Engelhard, M., Myers, A.L.: Comparison of experimental techniques for measuring isosteric heats of adsorption. Adsorption **6**, 275–286 (2000)

Siriwardane, R.V., Shen, M.S., Fisher, E.P., Paton, J.A.: Adsorption of CO_2 on molecular sieves and activated carbon. Energy Fuels **15**, 279–284 (2001)

Spencer, C.F., Danner, R.P.: Improved equation for saturated liquid density. J. Chem. Eng. Data **17**, 236–241 (1972)

Tlili, N., Grevillot, G., Ballieres, C.: Carbon dioxide capture and recovery by means of TSA and/or VSA. Int. J. Greenh. Gases Control. **3**, 519–527 (2009)

Valenzuela, D.P., Myers, A.L.: Adsorption equilibrium data handbook. Prentice-Hall, Englewood Cliffs (1989)

Wang, Y., LeVan, Y.D.: Adsorption equilibrium of carbon dioxide and water vapor on zeolite 5A and 13X and silica gel; pure components. J. Chem. Eng. Data **54**, 2839–2844 (2009)

Wang, Z.M., Arai, T., Kumagai, M.: Adsorption separation of low concentration of CO_2 and NO_2 by synthetic zeolites. Energy Fuels **12**, 1055–10660 (1998)